

Angular Distribution and Pulse Compression of Stimulated Raman Scattering in Ba(NO₃)₂ Crystal*

Chen Huiting^{1,2}, Lou Qihong¹, Dong Jingxing¹, Chen Wanchun³

¹ Shanghai Institute of Optics & Fine Mechanics, Chinese Academy of Sciences, Shanghai 201800

² Graduate School of the Chinese Academy of Sciences, Beijing 100039

³ Institute of Physics, Chinese Academy of Sciences, Beijing 100080

Abstract The high-efficiency SRS in barium nitrate (Ba(NO₃)₂) crystal was obtained pumped by a Q-switched Nd:YAG laser (532 nm) operated at 30 Hz. In the forward scattered direction, the first (563 nm), second (599 nm) and third (639 nm) Stokes pulses were presented, the radiation fields of which had cone structures with the scattered angles of 1.7°, 3.5° and 5.0°, respectively. Furthermore, it was pointed out that the angular distribution of Stokes radiation was independent of the pump intensity in this work. The results show that the angular distributions of SRS in Ba(NO₃)₂ crystals are mainly attributed to the phase matched process. The pulse widths of the pump, first, second and third Stokes pulses were measured to be 11.6 ns, 9.8 ns, 8.4 ns and 4.5 ns, respectively. This indicates that SRS in Ba(NO₃)₂ crystals can provide the possibility of effective pulse compression and increase of peak pulse intensity. With the pump intensity of about 150 W/cm², the maximum conversion efficiencies of the first, second and third Stokes pulses were 23.5%, 8.8% and 3.4%, respectively. Moreover, the saturation phenomenon of SRS efficiency was experimentally observed, which was due to the thermal loading in the Ba(NO₃)₂ crystal.

Keywords Stimulated Raman Scattering (SRS); Pulse compression; Angular distribution; Ba(NO₃)₂ crystal

CLCN TN248

Document Code A

0 Introduction

Stimulated Raman scattering (SRS) has been employed for more than 40 years as a method for frequency conversion of laser radiation to reach new spectral ranges. Solid-state materials, possessing favorable features for stimulated Raman scattering, have been of intense investigation by several world research group in last years^[1~3]. Their solid state nature, the compactness and robustness of solid state materials in comparison with large high-pressure gas-filled cells make them promising candidates for use in all-solid state laser systems^[4~6]. Among various solid-state Raman conversion media, the Ba(NO₃)₂ crystal has attached outstanding attention because of its high gain and strong mechanical properties^[7~9]. Recently, the Ba(NO₃)₂ crystal has been successfully applied to the Raman amplification of subpicosecond laser pulse^[10].

Although SRS has been obtained in more and

more crystalline materials recently, there are no detailed discussion on angular distribution and pulse compression of SRS in crystals. In this paper, the angular distributions and temporal profiles of the Stokes components were demonstrated in a Ba(NO₃)₂ crystal. The radiation fields of the first, second and third Stokes pulses had cone structures with the scattered angles of 1.7°, 3.5° and 5.0°, respectively. Moreover, their pulse widths were measured to be 11.6 ns, 9.8 ns, 8.4 ns and 4.5 ns, respectively. With the pump intensity of about 150 W/cm², the maximum conversion efficiencies of the first, second and third Stokes components were 23.5%, 8.8% and 3.4%, respectively.

1 The experimental setup

The schematic of the experiment setup is shown in Fig. 1. A-attenuator, F-filter, T-telescope, L₁, L₂, L₃-glass lens, Ba(NO₃)₂-Ba(NO₃)₂ Raman crystal, P₁, P₂-dispersing prisms, S₁-first Stokes, S₂-second Stokes, S₃-third Stokes, E₁, E₂-energy detector, SL-Slit. The Ba(NO₃)₂ crystal was grown with the aqua-solution cooling method by ourselves^[11]. It had a large size with the length of 48 mm and aperture of 10 mm × 10 mm. The Ba(NO₃)₂ crystal was cut along the [110] crystallographic axis and pumped by a Q-switched

*Supported by the National High Technology Project (No. 2004AA846020), by the National Science foundation (No. 10334110) and partly by the Shanghai Science & Technology Foundation

Tel: 021-69918629 Email: htchen4@yahoo.com.cn

Received date: 2005-12-19

Nd : YAG laser (532 nm) operated at 30 Hz. The pulse width of the Nd : YAG laser was 11.6 ns (FWHM) and the pulse energy was up to 600 mJ. The divergence angle of the pump beam was $\sim 360 \mu\text{rad}$ with a super-Gaussian pattern in near-field. The diameter of the collimated pump beam in the Raman crystal was 3 mm. The variable attenuator (A) was used for fine adjustment of the pump pulses energy, which was monitored by a calibrated energy meter (E_1). The telescope system T was composed of the glass lens (L_1) with 50 cm focal length and the glass lens (L_2) with 10 cm focal length. It was used to increase the pump laser intensity incident on the $\text{Ba}(\text{NO}_3)_2$ crystal. The highest pump intensity was limited by the optical damage threshold in the $\text{Ba}(\text{NO}_3)_2$ crystal, which is 10 J/cm^2 at the center of the pump-beam patterns. Behind the crystal, the scattered radiation was partially collimated by the lens (L_3) with 300 mm focal length. Afterwards, the radiation of Stokes components were separated by two flint glass dispersing prisms (P_1), (P_2) and the movable slit (SL). The scattered radiation energies of the Stokes components were measured by the energy detector (E_2). The temporal shapes of the Stokes components were recorded by a setup composed of a fast photodiode and digital oscillograph.

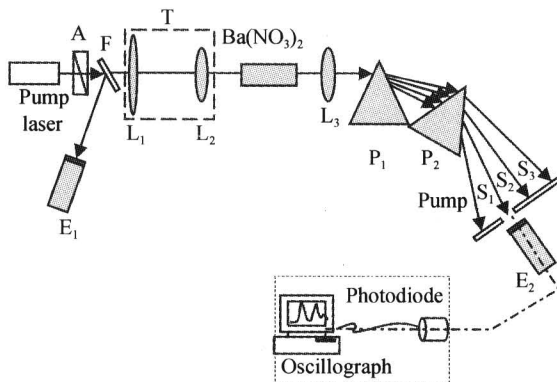


Fig. 1 The experimental setup of $\text{Ba}(\text{NO}_3)_2$ crystal stimulated Raman scattering

2 Results and discussion

The angular distribution of the scattered light was registered at a screen installed 1.5 m apart from the Raman shifter without any light splitting device behind the crystal. In the experiment, the radiation fields of Stokes components had spatial cone structures, the photograph of which at the screen is shown in Fig. 2. The first Stokes radiation in the $\text{Ba}(\text{NO}_3)_2$ crystal mostly traveled along the pump axis. The dark Ring 1 in Fig. 2 corresponds to the external border of the first Stokes radiation.

It was believed that the dark Ring 1 was due to the coupling of the first Stokes radiation with the pump radiation to create the second Stokes radiation by four-photo mixing. The included angle between the first Stokes radiation (external border) and the axis of pump laser was measured to be 1.7° (plane angle). The second and third Stokes scatterings under biharmonic excitation (pump + first Stokes component) had a rather broad cone structure. The second Stokes radiation was denoted with the orange Ring 2 in Fig. 2. The included angle between the second Stokes radiation (external border) and the axis of pump laser was 3.5° (plane angle). Likewise, the intense Ring 3 shown in Fig. 2 corresponded to the third Stokes radiation. The included angle between the third Stokes radiation (external border) and the axis of pump laser was 5.0° (plane angle). Furthermore, it didn't observe the dependence of the angular distribution of Stokes radiation on the pump intensity in the experiment. Because the angular distribution of Stokes radiation was independent of the pump intensity and the angles of the cones increased incrementally with the order of the Stokes components, it was believed that the angular distribution of SRS in $\text{Ba}(\text{NO}_3)_2$ crystal was mainly determined by the phase matched process.

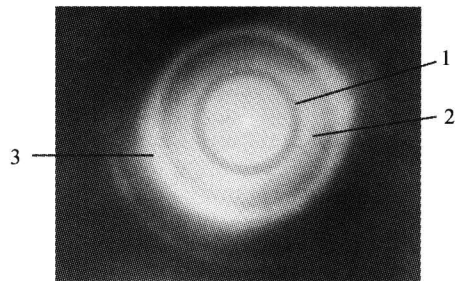


Fig. 2 The photograph of $\text{Ba}(\text{NO}_3)_2$ crystal stimulated Raman scattering at the screen

An optical spectrum analyzer (Ocean Optics HR2000 GR-UV-NIR) was used to measure the SRS spectrum. The wavelengths of pump, first, second and third Stokes pulses were 532, 563, 599 and 639 nm, respectively. It can be seen that the "breathing" vibration mode of the nitrate moiety (1047 cm^{-1}) dominates the frequency shift between the pump and Stokes radiations.

A 1.5 GHz LeCroy9362 digital oscilloscope with a 1 GHz DET210 fast photodiode was used to measure the profiles of the pump and the Stokes pulses, and the experimental results were shown in Fig. 4. The pulse widths of the pump, first, second and third Stokes pulses were 11.6 ns, 9.8 ns,

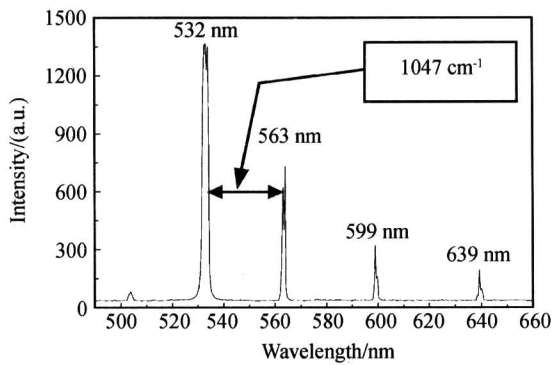


Fig. 3 Optical spectrum for SRS of Ba(NO₃)₂ crystal in single-pass experiment pumped by 532 nm pump laser

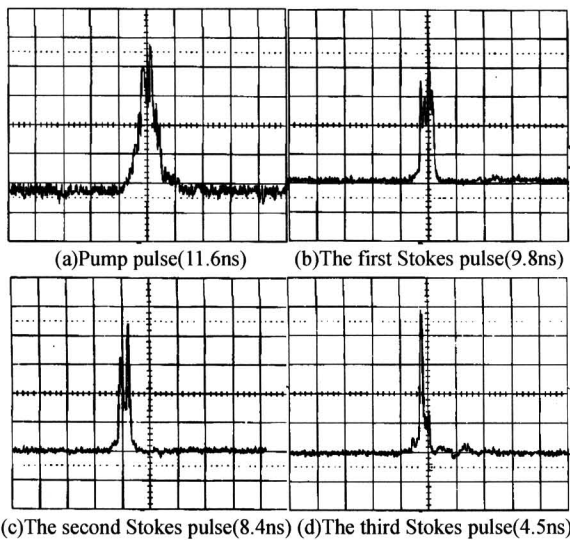


Fig. 4 Comparison of the temporal profiles of pump and Stokes components pulses; 20 ns/div

8.4 ns and 4.5 ns respectively. This indicates the possibility of effective pulse compression and increase of peak pulse intensity utilizing SRS in Ba(NO₃)₂ crystals.

The energies of the first, second and third Stokes components were presented as a function of the incident pump energy in Fig. 5. With the input pump energy of 581.4 mJ (pump intensity of 246.7 W/cm²), the output energies of the first, second and third Stokes pulses were 120.1 mJ, 39.2 mJ and 16.7 mJ, respectively. With the pump intensity of about 150 W/cm², obtained the maximum conversion efficiency of the Stimulated Raman scattering. The maximum conversion efficiencies of the first, second and third Stokes components were measured to be 23.5%, 8.8% and 3.4% respectively as shown in Fig. 6. A further increase in the pump intensity led to the saturation of SRS efficiency. This phenomenon may be caused by the thermal loading in the crystal which lowered the efficiency, since Raman processes always dissipate a fraction of the pump energy as phonon energy^[7].

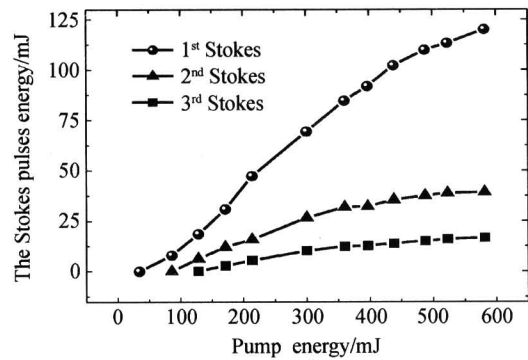


Fig. 5 Dependence of the output energies of the first, second and third Stokes components on the pump energy incident on the Ba(NO₃)₂ crystal

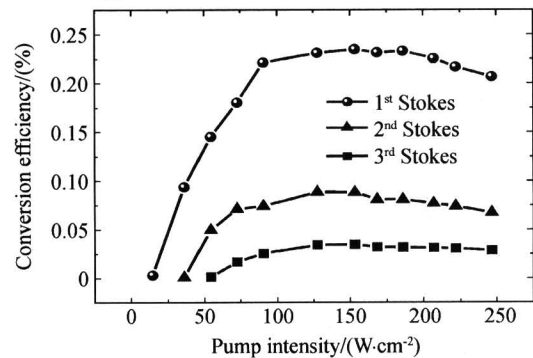


Fig. 6 Dependence of the conversion efficiencies of the first, second and third Stokes components on the pump intensity incident on the Ba(NO₃)₂ crystal

3 Conclusions

In summary, it has demonstrated the scattered angular distribution and the pulse compression of the first, second and third Stokes radiation in the Ba(NO₃)₂ crystal pumped by the 532 nm Nd:YAG laser. The scattered angles of the first, second and third Stokes radiation were measured to be 1.7°, 3.5° and 5.0°, respectively. The pump, first, second and third Stokes pulse widths were 11.6 ns, 9.8 ns, 8.4 ns and 4.5 ns, respectively. With the pump intensity of about 150 W/cm², the maximum conversion efficiency of the first (563 nm), second (599 nm) and third (639 nm) Stokes components were 23.5%, 8.8% and 3.4%, respectively. Moreover, the saturation phenomenon of SRS efficiency in the Ba(NO₃)₂ crystal was observed.

References

- 1 Basiev T T, Sobol A A, Zverev P G, et al. Comparative spontaneous Raman spectroscopy of crystals for Raman lasers. *Applied Optics*, 1999, **38**(3): 594~598
- 2 Kaminskii A A. Nonlinear-laser effects in $\chi^{(3)}$ - and $\chi^{(2)}$ -active organic single crystals. *JETP Lett*, 2003, **78**(10): 669~679
- 3 Mildren R P, Convery M, Pask H M, et al. Efficient all-solid-state, Raman laser in the yellow, orange and red. *Optics Express*, 2004, **12**(5): 785~790

- 4 Du Geguo, Ruan Shuangchen, Su Hongxin, *et al.* Studies on SRS spectra in single-mode silica fiber. *Acta Photonica Sinica*, 2004, **33**(8): 923~926
- 5 Sun Xiuping, Feng Kecheng, Zhang Xihe, *et al.* Study of polarized characters of stimulated Raman scattering spectrum in single mode circular fiber. *Acta Photonica Sinica*, 2005, **34**(8): 1169~1171
- 6 Xin Xiangjun, Yu Chongxiu, Zhang Ru, *et al.* The influence of configuration of Raman fiber amplifier on performance. *Acta Photonica Sinica*, 2003, **32**(2): 140~142
- 7 Takai N, Suzuki S, Kannari F. 20-Hz operation of an eye-safe cascade Raman laser with a $\text{Ba}(\text{NO}_3)_2$ crystal. *Appl Phys B*, 2002, **74**(6): 521~527
- 8 Grabtchikov A S, Lisinetskii V A, Orlovich V A, *et al.* Multimode pumped continuous-wave solid-state Raman laser. *Opt Lett*, 2004, **29**(21): 2524~2526
- 9 Simons J, Pask H, Dekker P, *et al.* Small-scale, all-solid-state, frequency-doubled intracavity Raman laser producing 5 mW yellow-orange output at 598 nm. *Opt Commun*, 2004, **229**(1-6): 305~310
- 10 Cheng W, Avitzour Y, Ping Y, *et al.* Reaching the nonlinear regime of Raman amplification of ultrashort laser pulses. *Phys Rev Lett*, 2005, **94**(4): 045003-1~045003-4
- 11 Chen W C, Liu D D, Zhang C L, *et al.* Larger $\text{Ba}(\text{NO}_3)_2/\text{Sr}(\text{NO}_3)_2$ crystal growth and solubility determination. *Mater Res Bull*, 2004, **39**(2): 309~316

$\text{Ba}(\text{NO}_3)_2$ 晶体受激拉曼散射的角度分布和脉冲压缩

陈慧挺^{1,2} 楼祺洪¹ 董景星¹ 陈万春³

(1 中国科学院上海光学精密机械研究所, 上海 201800)

(2 中国科学院研究生院, 北京 100039)

(3 中国科学院物理研究所, 北京 100080)

收稿日期: 2005-12-19

摘要 报道了利用重复频率为 30 Hz, 波长为 532 nm 的 Nd: YAG 倍频激光单次通过抽运硝酸钡 ($\text{Ba}(\text{NO}_3)_2$) 晶体(晶体由水溶液降温法生长, 长度为 48 mm, 横截面为 10 mm×10 mm), 获得高效率的一阶(563 nm), 二阶(599 nm)和三阶(639 nm)斯托克斯光的实验结果. 硝酸钡晶体沿着[110]晶轴方向切割. 观测到一、二、三阶斯托克斯光呈锥形环分布, 一、二、三阶斯托克斯光的散射外边缘与抽运光轴线间的夹角大小分别为 1.7°, 3.5°, 5.0°. 同时也观测到 $\text{Ba}(\text{NO}_3)_2$ 的 SRS 角度分布与抽运光强度无关. 定性分析认定, $\text{Ba}(\text{NO}_3)_2$ 的 SRS 角度分布主要是由相位匹配过程决定的. 测得抽运光、一、二、三阶斯托克斯光的脉宽分别为 11.6 ns, 9.8 ns, 8.4 ns 和 4.5 ns. 当抽运光功率密度约为 150 W/cm² 时, 获得一、二、三阶斯托克斯光的最大光光转换效率, 分别为 33.5%, 8.8% 和 3.4%. 此外, 由于晶体中的热沉积效应, 观察到了 $\text{Ba}(\text{NO}_3)_2$ 晶体的 SRS 转换效率饱和现象.

关键词 受激拉曼散射; 脉冲压缩; 角度分布; 硝酸钡晶体



Chen Huiting was born in 1981 in Dongyang, Zhejiang Province. He received his M. S. degree in Harbin Institute of Technology in 2004. Now he is a Ph. D. candidate at Shanghai Institute of Optics & Fine Mechanics, CAS. His major research interests include solid-state Raman lasers and fiber lasers.